THE FUEL CELL

An Ideal ChE Undergraduate Experiment

JUNG-CHOU LIN, H. RUSSELL KUNZ, JAMES M. FENTON, SUZANNE S. FENTON
University of Connecticut • Storrs, CT 06269

There is much interest in developing fuel cells for commercial applications. This interest is driven by technical and environmental advantages offered by the fuel cell, including high performance characteristics, reliability, durability, and clean power. A fuel cell is similar to a battery—it uses an electrochemical process to directly convert chemical energy to electricity. Unlike a battery, however, a fuel cell does not run down as long as the fuel is provided. Fuel cells are characterized by their electrolytes since the electrolyte dictates key operating factors such as operating temperature. The main features of five types of fuel cells are summarized in Table 1.[1]

TABLE 1
Summary of Fuel Cell Technologies

Fuel Cell	*Electrolyte*	*Temperature (°C)*	*Applications*
Alkaline (AFC)	Potassium Hydroxide	90-100	Military Space Flight
Phosphoric Acid (PAFC)	Phosphoric Acid	175-200	Electric Utility Transportation
Molten Carbonate (MCFC)	Lithium, Sodium, and/or Potassium Carbonate	650	Electric Utility
Solid Oxide (SOFC)	Zirconium Oxide Doped by Yttrium	1000	Electric Utility
Proton Exchange Membrane (PEMFC)	Solid polymer (poly-perfluorosulfonic acid)	<100	Electric Utility Portable Power Transportation

The proton exchange membrane (PEM) fuel cell is particularly amenable for use as an undergraduate laboratory experiment due to safety and operational advantages, including use of a solid polymer electrolyte that reduces corrosion, a low operating temperature that allows quick startup, zero toxic emissions, and fairly good performance compared to other fuel cells. A cross-sectional diagram of a single-cell PEM fuel cell is shown in Figure 1. The proton exchange membrane (Nafion®) is in contact with the anode catalyst layer (shown on the left) and a cathode catalyst layer (shown on the right). Each catalyst layer is in contact with a gas diffusion layer. The membrane, catalyst layers, and the gas diffusion layers make up what is called the membrane-electrode-assembly (MEA).

Fuel (hydrogen in this figure) is fed into the anode side of the fuel cell. Oxidant (oxygen, either in air or as a pure gas) enters the fuel cell through the cathode side. Hydrogen and oxygen are fed through flow channels and diffuse through gas diffusion layers to the

Jung-Chou Lin *earned his PhD from the University of Connecticut and his BS from the Tunghai University, Taiwan, both in chemical engineering. After graduation he was employed as an Assistant Professor in Residence to develop fuel cell experiments for the undergraduate laboratory at the University of Connecticut. Currently, he is a senior Research Engineer at Microcell Corporation in Raleigh, North Carolina.*

H. Russell Kunz *is Professor-in-Residence in the Chemical Engineering Department at the University of Connecticut and Director of Fuel Cell Laboratories at the University of Connecticut. An internationally recognized expert in fuel cell development, Dr. Kunz was educated at Rensselaer Polytechnic Institute, receiving his BS and MS degrees in Mechanical Engineering and his PhD in Heat Transfer*

James M. Fenton *is Professor of Chemical Engineering at the University of Connecticut. He teaches transport phenomena and senior unit operations laboratory courses. He earned his PhD from the University of Illinois and his BS from the University of California, Los Angeles, both in Chemical Engineering. His research interests are in the areas of electrochemical engineering and fuel cells.*

Suzanne S. Fenton *is the Assistant Department Head and Visiting Assistant Professor of Chemical Engineering at the University of Connecticut. She received her BS degree in Environmental Engineering from Northwestern University and her PhD in Chemical Engineering from the University of Illinois. She teaches transport phenomena and senior unit operations laboratory courses and provides innovative instruction for secondary school students.*

catalyst on their respective sides of the MEA. Activated by the catalyst in the anode, hydrogen is oxidized to form protons and electrons. The protons move through the proton exchange membrane and the electrons travel from the anode through an external circuit to the cathode. At the cathode catalyst, oxygen reacts with the protons that move through the membrane and the electrons that travel through the circuit to form water and heat.

Since the hydrogen and oxygen react to produce electricity directly rather than indirectly as in a combustion engine, the fuel cell is not limited by the Carnot efficiency. Although more efficient than combustion engines, the fuel cell does produce waste heat. The typical efficiency for a Nafion PEM fuel cell is approximately 50%.

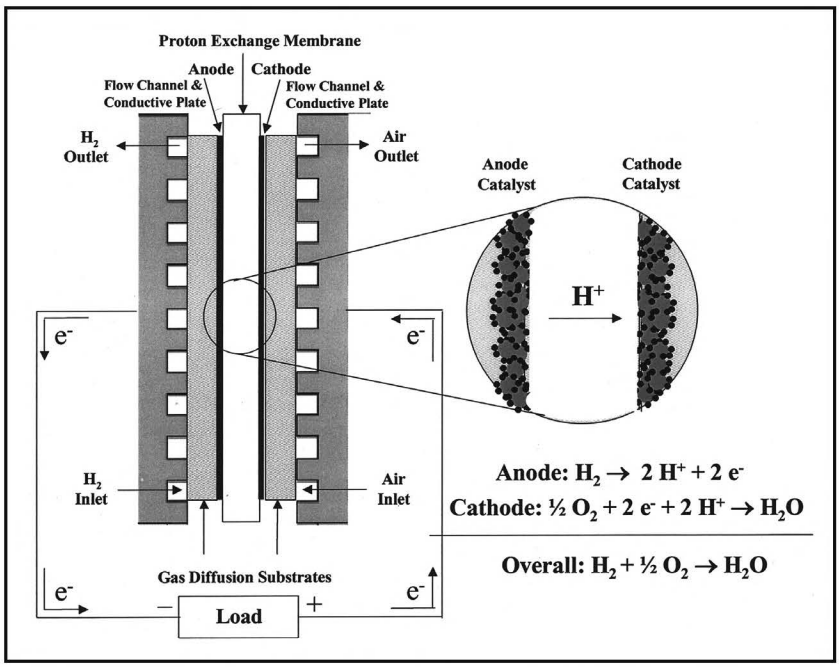

Figure 1. *PEM fuel cell cross section.*

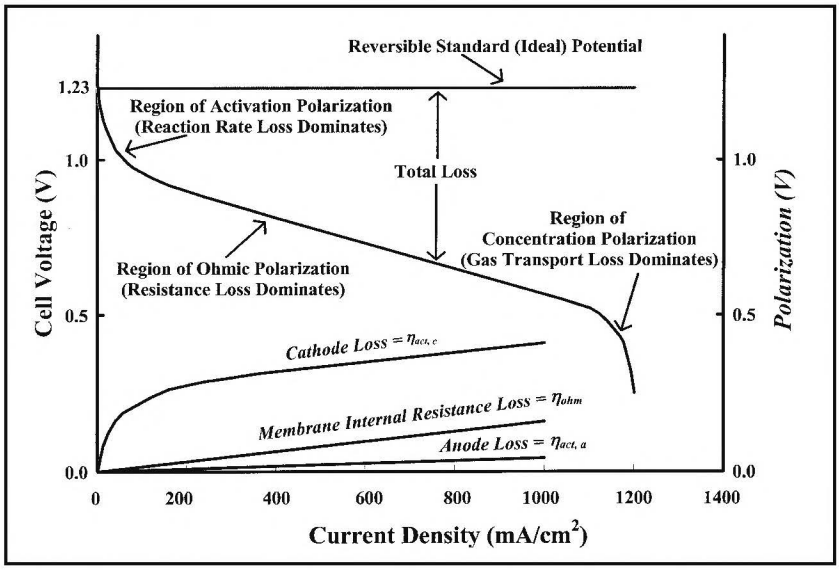

Figure 2. *Representative fuel cell performance curve at 25 °C, 1 atm.*

Fuel cells can be used to demonstrate a wide range of chemical engineering principles such as kinetics, thermodynamics, and transport phenomena. A general review of PEM fuel cell technology and basic electrochemical engineering principles can be found in the literature.[1-8] Because of their increasing viability as environmentally friendly energy sources and high chemical engineering content, fuel cell experiments have been developed for the chemical engineering undergraduate laboratory as described in the remainder of this paper.

OBJECTIVES

The objectives of the fuel cell experiment are

- *To familiarize students with the working principles and performance characteristics of the PEM fuel cell*
- *To demonstrate the effect of oxygen concentration and temperature on fuel cell performance*
- *To fit experimental data to a simple empirical model*

Students will measure voltage and membrane internal resistance as a function of operating current at various oxygen concentrations and temperatures; generate current density vs. voltage performance curves; and calculate cell efficiency, reactant utilization, and power density. Current density is defined as the current produced by the cell divided by the active area of the MEA. By fitting current density vs. voltage data to a simple empirical model, students can estimate ohmic, activation (kinetic), and concentration (transport) polarization losses and compare them to experimental or theoretical values.

BACKGROUND

The performance of a fuel cell can be characterized by its

1. *Current density versus voltage plot as shown in Figure 2*
2. *Efficiency*
3. *Reactant utilization (ratio of moles of fuel consumed to moles of fuel fed)*
4. *Power density (ratio of power produced by a single cell to the area of the cell (MEA)*

Current Density-Voltage Characteristics

Since a fuel cell is a device that facilitates the direct conversion of chemical energy to electricity, the ideal or best-attainable performance of a fuel cell is dictated only by the thermodynamics of the electrochemical reactions that occur (a function of the reactants and products). The electrochemical reactions in a hydrogen/oxygen fuel cell are shown in Eqs. (1) and (2).

Anode Reaction

$$H_2 \rightarrow 2H^+ + 2e^- \qquad (1)$$

Cathode Reaction

$$\frac{1}{2}O_2 + 2H^+ + 2e^- \rightarrow H_2O \qquad (2)$$

The reversible standard (*i.e.,* ideal) potential E° for the H_2/O_2 cell reaction is 1.23 volts per mole of hydrogen (at 25 °C, unit activity for the species, liquid water product) as determined by the change in Gibbs free energy. Reference 1 provides a derivation of this potential. The reversible standard potential for the hydrogen/oxygen cell is indicated on the current density-voltage diagram in Figure 2 as the horizontal line drawn at a voltage of 1.23. The Nernst equation can be used to calculate reversible potential at "non-standard" concentrations and a given temperature. Equation (3) is the Nernst equation specifically written for the H_2/O_2 cell based on the reactions as written.

$$E = E^\circ + \left(\frac{RT}{nF}\right)\ell n\frac{\left(P_{H_2}\right)\left(P_{O_2}\right)^{1/2}}{\left(P_{H_2O}\right)} \qquad (3)$$

where

- R gas constant (8.314 Joule/mol °K)
- T temperature (°K)
- F Faraday's constant (96,485 coulombs/equiv)
- n moles of electrons produced/mole of H_2 reacted (n=2 for this reaction)
- E° reversible potential at standard concentrations and temperature T (volts)
- E reversible potential at non-standard concentrations and temperature T (volts)
- P_{H2}, P_{O2}, P_{H2O} partial pressures of H_2, O_2, and H_2O, respectively (atm)

Note: 1 volt = 1 joule/coulomb

The Nernst equation cannot be used to make both temperature and concentration corrections simultaneously. To do this, one must first apply Eq. (4) to "adjust" the standard potential E° for temperature and then apply the Nernst equation to adjust for concentration at the new temperature.[6]

$$E_2^\circ - E_1^\circ = \frac{\Delta S}{nF}\left(T_2 - T_1\right) \qquad (4)$$

Subscripts 1 and 2 on E° denote "at temperatures T_1 and T_2" and ΔS is the entropy change of reaction (= - 163.2 J/°K for the H_2/O_2 reaction at 25 °C, unit activity for the species, liquid water product).

When a load (external resistance) is applied to the cell, nonequilibrium exists and a current flows. The total current passed or produced by the cell in a given amount of time is directly proportional to the amount of products formed (or reactants consumed) as expressed by Faraday's law

$$I = \frac{mnF}{sMt} \qquad (5)$$

where I (A) is the current, m (g) is the mass of product formed (or reactant consumed), n and F are defined above, s is the stoichiometric coefficient of either the product (a positive value) or reactant (a negative value) species, M (g/mol) is the atomic or molecular mass of the product (or reactant) species, and t (s) is the time elapsed. Equation (5) is valid for a constant current process. Faraday's law can be written in the form of the kinetic rate expression for H_2/O_2 cell as

$$\frac{I}{2F} = \frac{d(\text{moles } H_2O)}{dt} = \frac{-d(\text{moles } H_2)}{dt} = \frac{-2d(\text{moles } O_2)}{dt} \qquad (6)$$

There is a trade-off between current and voltage at nonequilibrium (nonideal) conditions. The current density-voltage relationship for a given fuel cell (geometry, catalyst/electrode characteristics, and electrolyte/membrane properties) and operating conditions (concentration, flow rate, pressure, temperature, and relative humidity) is a function of kinetic, ohmic, and mass transfer resistances. The current density vs. voltage curve shown in Figure 2 is referred to as the polarization curve. Deviations between the reversible potential and the polarization curve provide a measure of fuel cell efficiency.

Kinetic Limitations • Performance loss (voltage loss) resulting from slow reaction kinetics at either/both the cathode and anode surfaces is called activation polarization ($\eta_{act,c}$ and $\eta_{act,a}$). Activation polarization is related to the activation energy barrier between reacting species and is primarily a function of temperature, pressure, concentration, and electrode properties. Competing reactions can also play a role in activation polarization.

Kinetic resistance dominates the low current density portion of the polarization curve, where deviations from equilibrium are small. At these conditions, reactants are plentiful (no mass transfer limitations) and the current density is so small that ohmic (= current density x resistance) losses are negligible. The Tafel equation describes the current density-voltage polarization curve in this region.

$$\eta_{act} = B\log|i| - A \qquad (7)$$

where η_{act} is the voltage loss due to activation polarization (mV), i is current density (mA/cm^2), and constants A and B are kinetic parameters (B is often called the Tafel slope).[6]

As shown in Figure 2, the kinetic loss at the cathode, $\eta_{act,c}$ (the reduction of O_2 to form water) is much greater than kinetic loss at the anode, $\eta_{act,a}$, in the H_2/O_2 cell.

Ohmic Limitations • Performance loss due to resistance to the flow of current in the electrolyte and through the electrodes is called ohmic polarization (η_{ohm}). Ohmic polarization is described using Ohm's law (V=iR), where i is current density (mA/cm^2) and R is resistance (Ω-cm^2). These losses dominate the linear portion of the current density-voltage polarization curve as shown in Figure 2. Improving the ionic conductivity of the solid electrolyte separating the two electrodes can reduce ohmic losses.

Transport Limitations • Concentration polarization ($\eta_{conc,c}$ and $\eta_{con,,a}$) occurs when a reactant is consumed on the surface of the electrode forming a concentration gradient between the bulk gas and the surface. Transport mechanisms within the gas diffusion layer and electrode structure include the convection/diffusion and/or migration of reactants and products (H_2, O_2, H^+ ions, and water) into and out of catalyst sites in the anode and cathode. Transport of H^+ ions through the electrolyte is regarded as ohmic resistance mentioned above. Concentration polarization is affected primarily by concentration and flow rate of the reactants fed to their respective electrodes, the cell temperature, and the structure of the gas diffusion and catalyst layers.

The mass-transfer-limiting region of the current-voltage polarization curve is apparent at very high current density. Here, increasing current density results in a depletion of reactant immediately adjacent to the electrode. When the current is increased to a point where the concentration at the surface falls to zero, a further increase in current is impossible. The current density corresponding to zero surface concentration is called the limiting current density (i_{lim}), and is observed in Figure 2 at approximately 1200 mA/cm^2 as the polarization curve becomes vertical at high current density.

The actual cell voltage (V) at any given current density can be represented as the reversible potential minus the activation, ohmic, and concentration losses, as expressed in Eq. (8).

$$V = E - \left(\eta_{act,c} + \eta_{act,a}\right) - iR - \left(\eta_{conc,c} + \eta_{conc,a}\right) \qquad (8)$$

Note that activation ($\eta_{act,c}$, $\eta_{act,a}$) and concentration ($\eta_{conc,c}$, $\eta_{conc,a)}$ losses (all positive values in Eq. 8) occur at both electrodes, but anode losses are generally much smaller than cathode losses for the H_2/O_2 cell and are neglected. Ohmic losses (iR) occur mainly in the solid electrolyte membrane. An additional small loss will occur due to the reduction in oxygen pressure as the current density increases. Current fuel cell research is focused on reducing kinetic, ohmic, and transport polarization losses.

Cell Efficiency

Fuel cell efficiency can be defined several ways. In an energy-producing process such as a fuel cell, *current efficiency* is defined as

$$\varepsilon_f = \frac{\text{theoretical amount of reactant required to produce a given current}}{\text{actual amount of reactant consumed}} \qquad (9)$$

In typical fuel cell operation, current efficiency is 100% because there are no competing reactions or fuel loss. *Voltage efficiency* is

$$\varepsilon_V = \frac{\text{actual cell voltage}}{\text{reversible potential}} = \frac{V}{E} \qquad (10)$$

The actual cell voltage at any given current density is represented by Eq. (8) and reversible potential by Eq. (3). *Overall energy efficiency* is defined as

$$\varepsilon_e = \varepsilon_f * \varepsilon_v \qquad (11)$$

The H_2/O_2 fuel cell of Figure 2 operating at 0.8 V has a voltage efficiency of about 65% (=0.8/1.23*100). The overall efficiency at this voltage, assuming that the current efficiency is 100%, is also 65%. In other words, 65% of the maximum useful energy is being delivered as electricity and the remaining energy is released as heat (35%).

A fuel cell can be operated at any current density up to the limiting current density. Higher overall efficiency can be obtained by operating the cell at a low current density. Low current density operation requires a larger active cell area to obtain the requisite amount of power, however. In designing a fuel cell, capital costs and operating cost must be optimized based on knowledge of the fuel cell's performance and intended application.

Reactant Utilization

Reactant utilization and gas composition have major impact on fuel cell efficiency. Reactant utilization is defined as

$$U = \frac{\text{Molar flowrate}_{\text{reactant,in}} - \text{Molar flowrate}_{\text{reactant,out}}}{\text{Molar flowrate}_{\text{reactant,in}}} = \frac{\text{Mol } H_2 \text{ / s consumed}}{\text{Mol } H_2 \text{ / s fed}} \qquad (12)$$

"Molar flow rate consumed" in this equation is directly proportional to the current produced by the cell and can be calculated from Eq. (6). In typical fuel cell operation, reactants are fed in excess of the amount required as calculated by Faraday's law (*i.e.*, reactant utilization < 1). Higher partial pressures of fuel and oxidant gases generate a higher reversible potential and affect kinetic and transport polarization losses.

Power Density

The power density delivered by a fuel cell is the product of the current density and the cell voltage at that current density. Because the size of the fuel cell is very important, other terms are also used to describe fuel cell performance. Specific power is defined as the ratio of the power generated by a cell (or stack) to the mass of that cell (or stack).

EQUIPMENT, PROCEDURE, AND IMPLEMENTATION

The experiments presented here are designed to give the experimenter a "feel" for fuel cell operation and to demonstrate temperature and concentration effects on fuel cell performance. The manipulated variables are cell temperature, concentration of oxygen fed to the cathode, and current. Flow rates are held constant and all experiments are performed at 1 atm pressure. The measured variables are voltage and resistance, from which polarization curves are generated and fuel cell performance is evaluated. A simple empirical model can be fit to the data, allowing students to separately estimate ohmic resistance, kinetic parameters, and limiting current density. Table 2 summarizes the conditions investigated in this study.

Many other experimental options are available with the system described in this paper, including an investigation of the effect of 1) catalyst poisoning, 2) relative humidity of the feed gases, or 3) flow rate on fuel cell performance.

TABLE 2
Experimental Conditions: All at P=1 atm

Anode Feed			Cathode Feed		
Temp (°C)	*Flow rate (ml/min)*	*Dry basis Composition (Mole %)*	*Temp (°C)*	*Flow rate (ml/min)*	*Dry basis Composition (Mole %)*
80	98	100% H_2	80	376	100% O_2
80	98	100% H_2	80	376	Air-21% O_2 in N_2
80	98	100% H_2	80	376	10.5% O_2 in N_2
80	98	100% H_2	80	376	5.25% O_2 in N_2
18	98	100% H_2	18	376	100% O_2

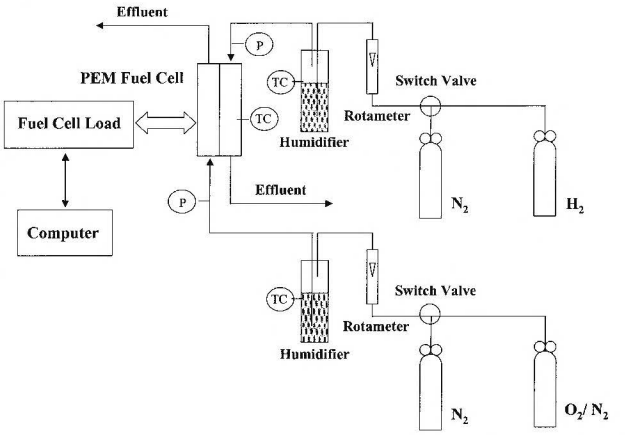

Figure 3. *Schematic of experimental setup.*

Equipment

A schematic diagram of the experimental setup is shown in Figure 3. An equipment list for in-house-built systems, including approximate cost and the names of several suppliers, is provided in Table 3. Completely assembled systems can be purchased from Scribner Associates, Inc. (www.scribner.com), Lynntech Inc. (www.lynntech.com), ElectroChem Inc. (www.fuelcell.com), and TVN (www.tvnsystems.com).

Hydrogen, supplied from a pressurized cylinder, is sent through the heated anode humidifier before being fed through heated tubes to the anode side of the fuel cell. Similarly, oxidant with any desired composition (oxygen

TABLE 3
Equipment List for In-House-Built Systems

Quant.	*Equipment/Supplies*	*Approx. Cost*	*Vendor**
1	Fuel cell load (sink and power supply)	$2,000	Scribner, Lynntech, Electrochem, TVN
1	Computer (optional)	$1,000	Dell, IBM, Compaq
1	Data acquisition card (optional)	$1,000	National Instruments
1	Single cell hardware w/heating element (5 cm^2)	$1,500	Electrochem, Fuel Cell Technology
1	Membrane-electrode-assembly (5 cm^2)	$200	Electrochem, Lynntech, Gore Associates
5	Temperature controller: 0-100°C	$1,000	OMEGA
4	Heating element (heating tape)	$400	OMEGA
5	Thermocouple	$200	OMEGA
2	Humidifier (2" ID stainless pipes and caps)	$200	McMaster-Carr
2	Rotameter (0-200 cc/min for H_2 fuel; 0-400 cc/min for oxidant)	$400	OMEGA
N/A	Valves and fittings (stainless steel)	$1,500	Swagelok
20 ft	Tubing (1/4" stainless steel)	$200	
4	Regulator	$1,000	Airgas
N/A	Gas (H_2, N_2, Air, O_2/N_2)	$1,000	Airgas
1	Digital flow meter (for calibration of rotameter)	$500	Humonics
	Other	$1,000	
	TOTAL	**~$13,000**	

**List is not exhaustive*

in nitrogen) is supplied from a pressurized cylinder and sent to the heated cathode humidifier before being fed through heated tubes to the cathode side of the fuel cell. Constant volumetric flow rates for anode and cathode feeds are manually controlled by rotameters. Humidification of the feed streams is necessary to maintain conductivity of the electrolyte membrane. Heating of the humidifiers, the tubes leading to the fuel cell, and preheating of the fuel cell is accomplished using heating tape, and temperatures of the feed streams and fuel cell are maintained using temperature controllers. To avoid flooding the catalyst structure, the humidifier temperature is maintained at or slightly below the cell temperature. The relative humidity of a stream exiting a humidifier can be determined manually by flowing the stream across a temperature controlled, polished metal surface and measuring its dew point. Effluent from the fuel cell is vented to a hood for safety purposes.

The PEM fuel cell comprises an MEA with an active area of 5 cm^2 (prepared at the University of Connecticut) and is housed in single-cell hardware with a single-pass serpentine flow channel. Our fuel cell load and data acquisition electronics are integrated in a single unit manufactured by Scribner Associates. During a typical experimental run (constant flow rate, oxidant composition, and temperature), the current is manipulated/adjusted on the fuel cell load and the voltage and resistance are read from built-in meters in the load. The fuel cell load uses the "current-interrupt technique"[3] to measure the total resistance between the two electrodes.

Procedure

A fuel cell with a prepared or commercial MEA is first connected to the fuel cell test system. Before feeding the hydrogen and oxidant into the fuel cell, humidified nitrogen is introduced to purge the anode and cathode sides of the single cell. During the purge (at 50 cc/min), the cell and humidifiers are heated to their respective operating temperatures (*e.g.*, cell, 80 °C, humidifiers, 80 °C). When the cell and humidifiers reach the desired temperature, the humidified nitrogen is replaced by humidified hydrogen and oxidant for the anode and cathode, respectively. During experiments, fuel and oxidant are always fed in excess of the amount required to produce a current of 1 A as calculated by Faraday's law (Eq. 5). The hydrogen and oxidant flow rates used in these experiments are based on operating at 1 A/cm^2 with an approximate reactant utilization of 45% for the hydrogen and 30% for oxidant (based on air). A sample calculation is provided in Table 4.

TABLE 4
Sample Flow-Rate Calculation

Faraday's Law: $\frac{m}{Mt} = \frac{Is}{nF}$ mol / time

Hydrogen consumption in fuel cell = I/(2F) mol/time
Oxygen consumption in fuel cell = I/(4F) mol/time
To produce a current of I = 1 Amp, H_2 consumption is:
= I/(2F) = 1/(2 x 96485) = $5.18 * 10^{-6}$ mol/s
= $3.11 * 10^{-4}$ mol/min

According to gas law: PV = NRT
At 80C and 1 atm, V/N = RT/P = 0.082*(273.15 + 80)/1 = 29 L/mol
So H_2 consumption is: V_{H2} = 9.0 ml/min @ 1 Amp current
O_2 consumption is: V_{02} = 4.5 ml/min @ 1 Amp current
Corresponding V_{air} = 4.5/0.21 = 21.4 ml.min @ 1 Amp current
To convert the above numbers to vol flowrates at a desired current density (amp/cm^2), divide ml/min by 1 cm^2 to get ml/min/cm^2.

For desired 45% H_2 utilization at 1 Amp/cm^2 current density
U = moles consumed/moles fed = 0.45
H_2 feed flow rate is: V_{H2} = 9.0/0.45 = 20 ml/min/cm^2 @ 1 Amp/cm^2
= 100 ml/min @ 1 A current with 5 cm^2 MEA

After introducing the fuel and oxidant into the cell, the open circuit voltage (zero current) should be between 0.8 and 1 volt. Fuel cell performance curves are generated by recording steady state voltage at different currents. Approximately 5 minutes is required to reach steady state for changes in current at constant composition and temperature, but it might take 20 to 30 minutes to reach steady state for a change in either oxidant composition or temperature. The system should be purged with nitrogen during shutdown. Short-circuiting the fuel cell will destroy the MEA.

Implementation and Assessment

This experiment will be included as part of a three-credit senior-level chemical engineering undergraduate laboratory. The course consists of two 4-hour labs per week, during which groups of 3 to 4 students perform experiments on five different unit operations throughout the semester (*e.g.*, distillation, heat exchanger, gas absorption, batch reactor, etc.). Each unit is studied for either one or two weeks, depending on the complexity and scale of the equipment. Given only general goals for each experiment, students are required to define their own objectives, develop an experimental plan, prepare a pre-lab report (including a discussion of safety), perform the experiments, analyze the data, and prepare group or individual written and/or oral reports.

The fuel cell experiment described above can easily be completed in one week (two 4-hour lab periods). Additional experiments can be added to convert this lab into a two-week experiment. Due to their similar nature and focus (generation of performance/characteristic curves and analysis of efficiency at various operating conditions), the fuel cell experiment could be used in place of the existing centrifugal pump experiment.

Immediate assessment of the experiment will be based on student feedback and student performance on the pre-lab presentation, lab execution, and technical content of the written/oral reports. Existing assessment tools (End-of-Course Survey, Senior Exit Interview, Alumni Survey, Industrial Advi-

sory Board input, and annual faculty curriculum review) will be used to evaluate the overall impact of the experiment.

RESULTS AND DISCUSSION

Performance

Performance curves (voltage vs. current density) and membrane resistance vs. current density at 80 °C with different oxidant compositions (pure oxygen, air, 10.5% O_2 in N_2 and 5.25% O_2 in N_2) are shown in Figure 4. Measured open circuit voltage (V_{oc}) can be compared to reversible potential calculated via Eqs. (3) and (4). These values are presented in the legend of Figure 4. Students will observe that the actual open circuit voltage is slightly lower than the theoretical maximum potential of the reactions. Activation polarization (kinetic limitation) is observed at very low current density (0-150 mA/cm^2). Kinetic losses increase with a decrease in oxygen concentration. At low current densities, membrane resistance (ohmic polarization) is nearly constant (about 0.14 Ω-cm^2) and is independent of oxidant composition. Membrane resistance begins to increase slightly with increasing current density at 800 mA/cm^2 due to dry-out of the membrane on the anode side. Dry-out occurs at high current density because water molecules associated with migrating protons are carried from the anode side to the cathode at a higher rate than they can diffuse back to the anode. Mass transport limitations due to insufficient supply of oxygen to the surface of the catalyst at high current density is observed, especially for gases containing low concentrations of oxygen. Limiting currents are evident at about 340 mA/cm^2 and 680 mA/cm^2 for the 5.25% and 10.5% oxygen gases, respectively, but are not obvious for pure oxygen and air. Limiting current density can be shown to be directly proportional to oxygen content.

The effect of operating temperature (18°C vs. 80°C, both at 100% relative humidity) on cell performance and membrane resistance for a pure O_2/H_2 cell is shown in Figure 5. Measured open-circuit voltage and reversible potential at 80°C are slightly lower than the corresponding voltages at 18°C. This is due to higher concentrations of reactants when fed at lower temperatures and 100% relative humidity. Elevated temperatures favor faster kinetics on the catalyst surface and lower membrane resistance, however, resulting in better cell performance. Under fully hydrated environments (100% RH), membrane resistance decreases with increasing temperature due to increased mobility of the protons. Again, limiting current density for pure oxygen is not obvious in this plot.

A linear relationship between current density and reactant utilization (per Eq. 5) is clearly evident in Figure 6. Reactant utilization decreases with increasing inlet oxygen concentration (at constant flow rate) because of an increase in the moles reactant feed.

Power density (W/cm^2) delivered by a fuel cell is defined by the product of current density drawn and voltage at that current density. The effect of current density on power density for various oxidant compositions is shown in Figure 7. For a given feed composition, maximum power density is achieved approximately halfway between no-load and limiting current densities. The selection of "optimal" operating

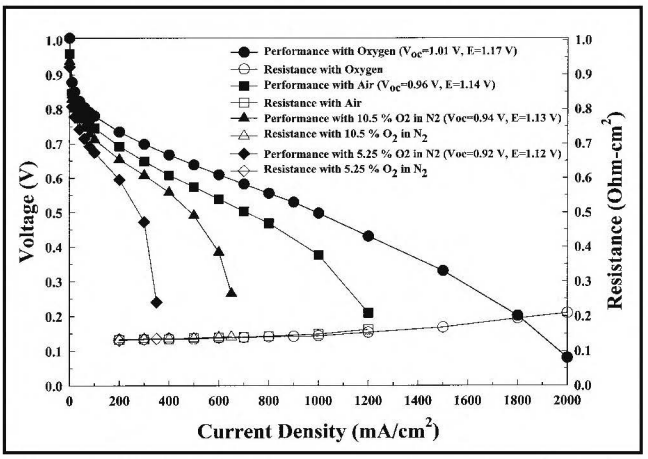

Figure 4. *Effect of oxidant concentration on cell performance and membrane resistance at 80°C, 1 atm.*

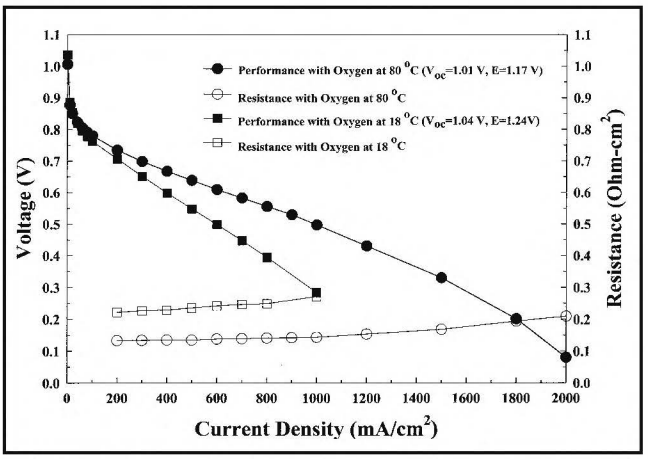

Figure 5. *Effect of temperature on cell performance and membrane resistance at 1 atm, pure O_2.*

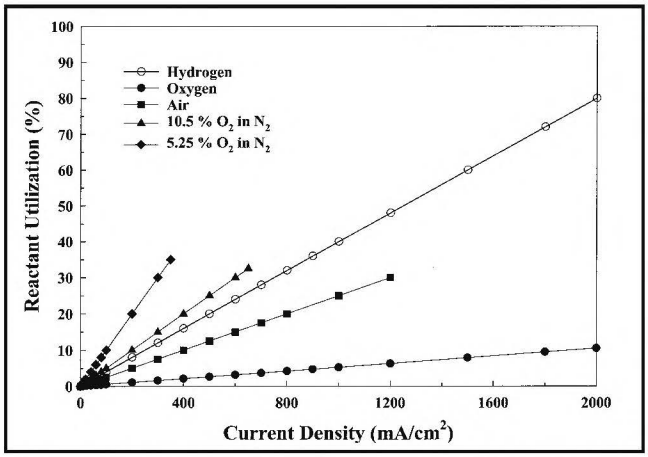

Figure 6. *Effect of current density and oxidant composition on reactant utilization at 80°C, 1 atm.*

conditions depends on how the fuel cell is to be used. For example, for vehicular applications, higher power density is required to minimize the weight of the car at the expense of efficiency. For residential (non-mobile) applications, a cell with higher efficiency would be preferred.

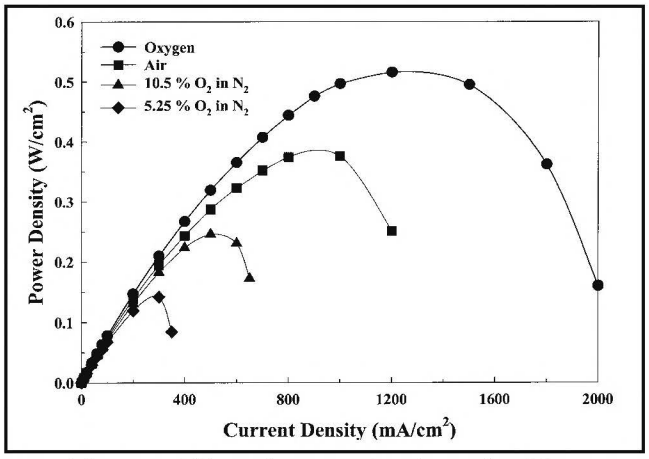

Figure 7. *Effect of current density and oxidant composition on power density at 80°C, 1 atm.*

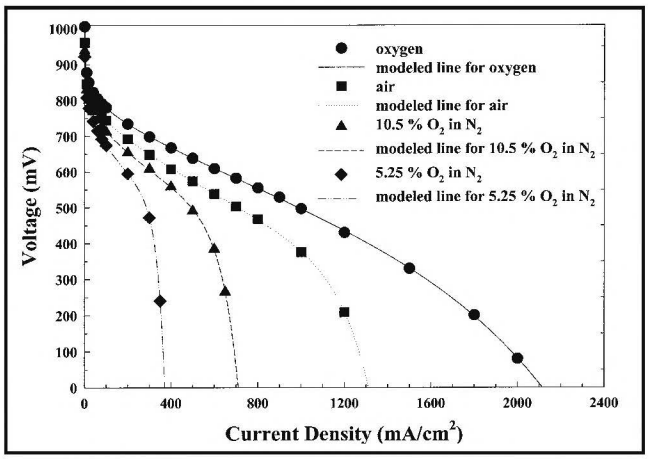

Figure 8. *Nonlinear regression fit of experimental data at 80°C, 1 atm.*

Empirical Model

Although comprehensive modeling of a fuel cell system is beyond the scope of an undergraduate lab, a simple model describing voltage-current characteristics of the fuel cell can be introduced to the students and tested for 1) its ability to fit the data, and 2) its usefulness as an analytical tool. The following empirical model describing the loss of cell voltage due to kinetic, ohmic, and transport limitations was proposed by Srinivasan, *et al.*:[9]

$$V = E - (B \log(i) - A) - iR - w \exp(zi) \qquad (13)$$

where E, B, A, R, w, and z are "fit" parameters. Lumping E and A together gives

$$V = E + A - (B \log(i)) - iR - w \exp(zi) \qquad (14)$$

Equation (14) is modeled after Eq. (8) assuming the anode polarization terms in Eq. (8) are negligible, that the kinetic limitations of the cathode can be described by the Tafel Eq. (7), and that mass transport losses can be fit using the parameters w and z. The purely empirical term, w exp(zi), in Eq. (14) can be replaced with a more physically meaningful term

$$C \log\left(\frac{1}{1-\frac{i}{i_{lim}}}\right) \qquad (15)$$

where i_{lim} (mA/cm^2) is the current density corresponding to a zero surface concentration, and C (mV/decade) is a parameter related to the Tafel slope. Due to space limitations, however, the physical meanings and the accurate estimation of C and i_{lim} will be explained in a forthcoming publication.[10]

The model fit to experimental data using nonlinear regression software (Polymath) is shown in Figure 8. All curves generated using this model have correlation coefficients in excess of 0.999. The model therefore is excellent as a fitting function for fuel cell performance curves from which values can be interpolated or extrapolated. This is particularly handy for estimating limiting current density in cases where the data is insufficient.

Values for the adjustable parameters [(E+A), B, R, w, z] calculated by the regression software are summarized in Table 5. The "regression generated" values for R can be compared to experimentally measured values (shown on the right-hand scale of Figures 4 and 5) and "regression generated" values for B can be compared to those predicted using theory. In this way the model can be tested for its "analytical" capability.

TABLE 5
Best-Fit Values for Kinetic Parameters, Ohmic Losses, and Transport Parameters Obtained Using Eq. (14) Compared to Values Calculated or Measured by Other Means

Eq. (14): $V = E + A - (B \log(i)) - iR - w \exp(zi)$

Eq. (7): $\eta_{act} = B \log|i| - A$

Oxidant Comp	*Temp (°C)*	*E + A (mV)*	$B_{fit\ to\ Eq.\ 14}$ *(mV/dec)*	$B_{fit\ to\ Eq.\ 7}$ *(mV/dec)*	$R_{fit\ to\ Eq.\ 14}$ *(Ω-cm²)*	$R_{measured}$ *(Ω-cm²)*	*w (mV)*	*z (cm²/mA)*	*Correlation Coefficient (R^2)*
Oxygen	80	963	79	85	0.20	0.14 - 0.16	4.202	0.0020	0.999
Air	80	927	77	84	0.29	0.14 - 0.16	0.018	0.0074	0.999
10.5% O_2 in N_2	80	921	87	94	0.33	0.14 - 0.16	0.035	0.0133	0.999
5.25% O_2 in N_2	80	902	88	95	0.51	0.14 - 0.16	0.008	0.0297	0.999

Contrary to experimental results, resistance calculated using Eq. (14) increases with decreasing oxygen concentration and is 40%-200% higher than measured membrane resistance (0.14 - 0.16 Ω-cm^2 measured by the current-interrupt technique). This suggests that R from Eq. (14) includes voltage losses other than the ohmic resistance of the membrane and that the model is not reliable in predicting true physical behavior of individual contributions to the polarization curve. For instance, "model R" is assumed to be constant over the entire range of current densities, but in actual fuel cell operation, R is a function of current density at high current density.

Theoretical Tafel slope, B, is equal to 2.303 RT/α_aF where R is the ideal gas constant, T is absolute temperature, F is Faraday's constant, and α_a is a lumped kinetic parameter equal to 1 for the oxygen reduction reaction occurring on the cathode.[6] According to this theory, the Tafel slope should be about 70 mV/decade at 80°C. Table 5 shows the regression generated B is 20-36% higher than the value of 70 mV/decade. Again, one might suggest some physical reasons for this discrepancy, such as the existence of diffusion or resistive losses in the cathode catalyst layer of the electrode. We may argue, however, that the model is too "flexible" to assign any physical significance to the values of the "fit" parameters (*i.e.*, a huge range of values for each parameter will yield a good fit).

Tafel slopes are more accurately obtained from raw data using the Tafel equation, Eq. (7). In this case, B can be found by plotting iR-free voltage (V + iR) vs. log i (see Figure 9) and measuring the slope of the line in the kinetically controlled portion of the plot (at low values of log i). Values for B found by using this technique have been included in Table 5. While those values found from Eq. (7) are more accurate than those from Eq. (14), they still differ from the theoretical value of 70.

The Tafel slope should not be a function of the oxygen concentration at low current density, so the lines in Figure 9 should all be parallel. It is clear that mass transport does not interfere with the calculation for the oxygen performance (straight line over the full decade of 10 to 100 mA/cm^2). The 5.25% oxygen curve, however, is linear only for two points, 10 and 20 mA/cm^2, as mass transport resistances occur at lower current densities.

The parameters w and z are intended to describe mass transport limitations, but actually have no physical basis. One might expect these parameters to be dependent on flow characteristics in the cell that were not investigated in this study. Therefore, the predictive or analytical usefulness of w and z cannot be evaluated.

CONCLUSIONS

Fuel-cell based experiments embody principles in electrochemistry, thermodynamics, kinetics, and transport, and are well suited for the chemical engineering curricula. Students are given an opportunity to familiarize themselves with fuel cell operation and performance characteristics by obtaining voltage-versus-current-density data for the unit at varying oxidant compositions and temperatures.

A simple model can be used as a fitting function for interpolation and extrapolation purposes. Model sensitivity analysis can be performed to evaluate its usefulness as an analytical tool. The lab can be completed easily in two 4-hour lab periods. The experiment is also suitable for use as a demonstration in a typical lecture course or as a hands-on project for high school students and teachers. The experimental system is described, including cost and vendor information.

NOMENCLATURE

A	kinetic parameter used in Eqs. (7), (13), and (14) (mV)
B	Tafel slope (mV/decade)
C	parameter related to the Tafel slope (mV/decade)
E	reversible potential at nonstandard concentration at temperature T (V or mV)
E^0	reversible potential at standard concentration at temperature T (V or mV)
F	Faraday's constant = 96,485 (coulombs/equivalent)
I	current (A)
i	current density (mA/cm^2)
i_{lim}	limiting current density (mA/cm^2)
M	molecular weight (g/mol)
m	mass of product formed or reactant consumed (g)
n	moles of electrons participating in the reaction per mole of reactant (equiv/mol)
N	moles
P_{H2},P_{O2},P_{H2O}	partial pressures (atm)
R	electrical resistance (Ω-cm^2)

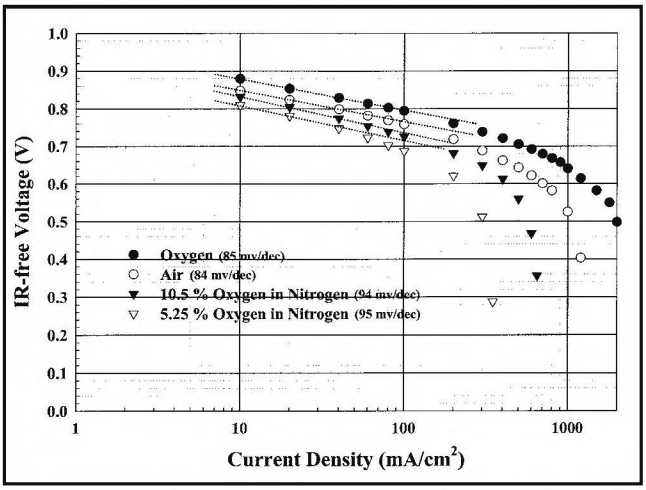

Figure 9. *Tafel slope estimation using IR-free voltage plot of experimental data at 80°C, 1 atm.*

R	universal gas constant = 8.31 (J/mol-K)
s	Stoichiometric coefficient of the product (positive value) or reactant (negative value) species
ΔS	entropy change of reaction (J/K)
T	temperature (K)
t	time (s)
U	reactant utilization (moles consumed/moles fed)
V	voltage (V or mV)
w	mass transport parameter used in Eqs. (13) and (14) (mV)
z	mass transport parameter used in Eqs. (13) and (14) (cm^2/mA)
α_a	a lumped kinetic parameter equal to 1 for the oxygen reduction reaction
ε_e	overall energy efficiency = current efficiency * voltage efficiency
ε_f	current efficiency = theoretical reactant required/ amount of reactant consumed (g/g)
ε_v	voltage efficiency = actual cell voltage/reversible potential (V/V)
$\eta_{act,a}$,$\eta_{act,c}$	activation polarization at the anode and cathode, respectively (mV)
$\eta_{conc,a}$,$\eta_{conc,c}$	concentration polarization at the anode and cathode, respectively (mV)

REFERENCES

1. Thomas, S., and M. Zalbowitz, *Fuel Cells: Green Power* Los Alamos National Laboratory, LA-UR-99-3231 (1999); downloadable PDF file available at <http://education.lanl.gov/resources/fuelcells/>
2. Larminie, J., and A. Dicks, *Fuel Cell Systems Explained,* John Wiley & Sons, New York, NY (2000)
3. Hoogers, G., *Fuel Cell Technology Handbook,* 1st ed., CRC Press (2002)
4. Hirschenhofer, J.H., D.B. Stauffer, R.R. Engleman, and M.G. Klett, *Fuel Cell Handbook,* 5th ed., National Technical Information Service, U.S. Department of Commerce, VA (2000)
5. Koppel, T., and J. Reynolds, *A Fuel Cell Primer: The Promise and the Pitfalls,* downloadable PDF file available at <www.fuelcellstore.com/cgi-bin/fuelweb/view=item/cat=18/subcat=19/product=20>
6. Prentice, G., *Electrochemical Engineering Principles,* Prentice Hall, New Jersey (1991)
7. Bard, A.J., and L. Faulkner, *Electrochemical Methods: Fundamentals and Applications,* 2nd ed., John Wiley & Sons, New York, NY (2000)
8. Fuel Cells 2000 Index Page, The Online Fuel Cell Information Center at <www.fuelcells.org>
9. Kim, J., S-M. Lee, and S. Srinivasan, "Modeling of Proton Exchange Membrane Fuel Cell Performance with an Empirical Equation," *J. Electrochem. Soc.,* **142**(8), 2670 (1995)
10. Williams, M.V., H.R. Kunz, and J.M. Fenton, "Evaluation of Polarization Sources in Hydrogen/Air Proton Exchange Membrane Fuel Cells," to be published in *J. Electrochemical Society* ❐

Nanostructured Materials

Continued from page 37.

and results of peer evaluation.

CONCLUSION

ZSM-5 synthesis serves as an excellent example to introduce students to the basic concepts of templated synthesis and self-assembly that govern nanomaterials synthesis. This experiment brings together a number of subjects that students have learned from their previous courses: infrared spectroscopy (from organic chemistry), kinetic analysis and reactor operation (from reaction engineering), heat transfer (from transport phenomena), and phase behavior (from thermodynamics). The project also requires students to demonstrate their creativity and innovation through the experimental design and implementation of a nanostructured material synthesis.

ACKNOWLEDGMENTS

This work was supported by the NSF Grant CTS 9816954 and the Ohio Board of Regents Grant R5538.

REFERENCES

1. Gates, B.C., *Catalytic Chemistry,* John Wiley & Sons (1992)
2. Breck, D.W., *Zeolite Molecular Sieves: Structure, Chemistry, and Use,* John Wiley & Sons (1973)
3. Dyer, A., *An Introduction to Zeolite Molecular Sieves,* John Wiley & Sons (1988)
4. Kerr, G.T., *Catal. Rev. - Sci. Eng.,* **23**, 281 (1981)
5. Kerr, G.T., *Sci. Am.,* **261**, 100 (1989)
6. Thomas, J.M., *Sci. Am.,* **266**, 112 (1992)
7. Burkett, S.L., and M.E. Davis, *Chem. Mater.,* 7, 920 (1995)
8. Kirschhock, C.E.A., V. Buschmann, S. Kremer, R. Ravishankar, C.J.Y. Houssin, B.L. Mojet, R.A. van Santen, P.J. Grobet, P.A. Jacobs, and J.A. Martens, *Angew. Chem., Int. Ed.,* **40**, 2637 (2001)
9. Kresge, C.T., M.E. Leonowicz, W.J. Roth, J.C. Vartuli, and J.S. Beck, *Nature,* **359,** 710 (1992)
10. Beck, J.S., J.C. Vartuli, W.J. Roth, M.E. Leonowicz, C.T. Kresge, K.D. Schmitt, C.T.W. Chu, D.H. Olson, E.W. Sheppard, et al., *J. Am. Chem. Soc.,* **114**, 10834 (1992)
11. Sayari, A., and S. Hamoudi, *Chem. of Mats.,* **13**, 3151 (2001)
12. Ying, J.Y., C.P. Mehnert, and M.S. Wong, *Angew. Chem., Int. Ed. Engl.,* **38**, 56 (1999)
13. Corma, A., *Chem. Revs.,* **97**, 2372 (1997)
14. Konduru, M.V., S.S.C. Chuang, and X. Kang, *J. Phys. Chem. B.,* **105**, 10918 (2001)
15. Monnier, A., F. Schuth, Q. Huo, D. Kumar, D. Margolese, R.S. Maxwell, G.D. Stucky, M. Krishnamurty, and P. Petroff, *Science,*, **261**, 1299 (1993)
16. Huo, Q., R. Leon, P.M. Petroff, and G.D. Stucky, *Science,* **268**, 1324 (1995)
17. Kim, J.M., and G.D. Stucky, *Chem. Commun.,* **13,** 1159 (2000)
18. Kresge, C.T., M.E. Leonowicz, W.J. Roth, J.C. Vartuli, and J.S. Beck, *Nature,* **359**, 710 (1992)
19. Konduru, M.V., and S.S.C. Chuang, *J. Catal.,* **196**, 271 (2000)
20. Kruk, M., M. Jaroniec, V. Antochshuk, and A. Sayari, *J. Phys. Chem., B,* **106**, 10096 (2002)
21. Treacy, M.M.J., and J.B. Higgins, *Collection of Simulated XRD Powder Patterns of Zeolites,* Elsevier (2001)
22. Coudurier, G., C. Naccache, and J. Vedrine, *J. Chem. Soc., Chem. Commun.,* 1413 (1982) ❐